

First observation of quasi-monoenergetic electron bunches driven out of ultra-thin diamond-like carbon (DLC) foils

D. Kiefer^{1,2,a}, A. Henig^{1,2}, D. Jung^{1,2}, D.C. Gautier³, K.A. Flippo³, S.A. Gaillard^{3,4,5}, S. Letzring³, R.P. Johnson³, R.C. Shah³, T. Shimada³, J.C. Fernández³, V.Kh. Liechtenstein^{2,6}, J. Schreiber^{1,2,7}, B.M. Hegelich^{2,3}, and D. Habs^{1,2}

¹ Max-Planck-Institut für Quantenoptik, Hans-Kopfermann-Str. 1, 85748 Garching, Germany

² Fakultät für Physik, Ludwig-Maximilians-Universität München, Coulombwall 1, 85748 Garching, Germany

³ Los Alamos National Laboratory, Los Alamos, New Mexico 87545, USA

⁴ Department of Physics, MS-220, University of Nevada, Reno, 89557 Nevada, USA

⁵ Forschungszentrum Dresden Rossendorf, Bautzner Landstrasse 128, 01328 Dresden, Germany

⁶ RRC Kurchatov Institute, 123182 Moscow, Russia

⁷ Blackett Laboratory, Imperial College London, London SW7 2AZ, United Kingdom

Received 30 November 2008 / Received in final form 3 March 2009

Published online 9 July 2009 – © EDP Sciences, Società Italiana di Fisica, Springer-Verlag 2009

Abstract. Electrons have been accelerated from ultra-thin diamond-like carbon (DLC) foils by an ultrahigh-intensity laser pulse. A distinct quasi-monoenergetic electron spectrum peaked at 30 MeV is observed at a target thickness as thin as 5 nm which is in contrast to the observations of wide spectral distributions for thicker targets. At the same time, a substantial drop in laser-accelerated ion energies is found. The experimental findings give first indication that relativistic electron sheets can be generated from ultra-thin foils which in future may be used to generate brilliant X-ray beams by the coherent reflection of a second laser.

PACS. 52.38.-r Laser-plasma interactions – 52.38.Kd Laser-plasma acceleration of electrons and ions – 52.50.Jm Plasma production and heating by laser beams – 41.75.Jv Laser-driven acceleration

1 Introduction

The interaction of ultra-high intensity laser pulses with matter has opened new ways to generate relativistic electron bunches up to GeV energies by bubble formation in a plasma [1–3]. Besides the efficient electron acceleration, electron dynamics during the laser plasma interaction have been exploited to generate incoherent multi-keV X-rays [4]. A different approach is the coherent scattering of laser photons with energy $\hbar\omega_0$ off a dense electron sheet with electron energies $E_e = \gamma mc^2$. Counter propagating photons reflected off such a relativistic electron mirror would experience an energy upshift to $4\gamma^2\hbar\omega_0$ [5], opening the route towards compact, intense brilliant X-ray sources with ultra-short pulse duration [6].

Different schemes exist to realize such relativistic mirrors. A technique recently demonstrated is to utilize the electron density spike of a wake wave generated by the propagation of a laser pulse in an underdense plasma [7]. Here, coherent scattering with $\gamma \approx 5$ was shown experimentally [8,9]. However, the scaling up to higher γ values may be difficult, as this involves a decrease in plasma density, corresponding to large mirror structures. Alterna-

tively, high harmonics up to the keV level have been generated from a relativistic oscillating plasma layer near the critical surface, induced by the interaction of a solid density target with a linear polarized laser [10]. Here, a very broad spectral bandwidth is inherently generated due to the ultra-short velocity spike at which coherent emission only sets in [11–13]. A classical FEL can also be regarded as a relativistic electron mirror, where the magnetic undulator field is reflected by a sequence of relativistic electron micro-bunches.

A new concept is the generation of a very dense relativistic electron sheet induced by the interaction of a high intensity laser pulse with an ultra-thin foil [14,15]. In contrast to thicker targets, ultra-thin foils discussed in this paper (sub 10 nm), are ab initio partially transparent to the laser, as the collisionless laser skin depth is of the same order as the foil thickness. Here, electrons can be pushed out of the foil very effectively if the laser field is stronger than the static electric field, built up by the charge separation of the electrons and ions [6,16]. Owing to the ultra-short, high density characteristic of the generated electron bunches this new scheme of electron acceleration using ultra-thin solid density targets inherently results in large electron currents I which may be significantly higher than any so far achieved in the laser bubble

^a e-mail: daniel.kiefer@mpq.mpg.de

acceleration mechanism. Such ultra-high currents are essential for laser driven *coherent* X-ray sources, as the so called Pierce parameter, which controls the properties of an FEL, scales with $I^{1/3}$ [17,18]. In our case the chain of micro-bunches of a classical FEL is replaced by a single intense micro-bunch, the reflecting mirror. This reflection off a relativistic electron mirror with density close to a solid target, may give great opportunity to obtain coherent keV X-rays within a relatively narrow bandwidth.

In this paper, we report on the electron characteristics observed at the interaction of an ultra-intense laser pulse with a 5 nm DLC foil. First, we present the experimental setup, followed by the results. The experimental findings are discussed, and a brief outlook is finally given.

2 Experiment

The experimental investigation of the regime discussed here is quite demanding, as the main ingredients being: (1) a high intensity laser pulse, strong enough to separate a majority of the electrons from the ions, (2) ultra-thin foils (<10 nm), resistant to inevitable laser induced target preheating, (3) an ultra-high laser pulse contrast which enables the interaction of the main pulse with an undisturbed foil.

The experiment was performed at the Trident laser facility at the Los Alamos National Laboratory (LANL). The Trident short pulse laser beam delivered ~ 90 J within a 500 fs pulse at a central wavelength of $\lambda_L = 1.053$ μm . The linear polarized beam was focused by a $f/3$ off-axis parabolic mirror to a 9.4 μm FWHM focal spot [19], resulting in a laser peak intensity of $I_L = 2 \times 10^{20}$ W/cm^2 , equivalent to a normalized laser vector potential of $a_L \sim 12$, with $a_L^2 = I_L [\text{W}/\text{cm}^2] \lambda^2 [\mu\text{m}^2] / 1.37 \times 10^{18}$.

Ultra-thin DLC foils with thicknesses ranging from 3 nm to 58 nm were irradiated under normal incidence with linear polarized light. DLC is a quasi-amorphous carbon state consisting of both diamond and graphite crystal-lite structure. Nowadays, it can be produced with a high portion of sp^3 -bond content, showing exceptional diamond like properties, i.e. transparency, high mechanical strength and radiation hardness. These outstanding features make them ideal for laser applications. For the presented experiment, we used DLC foils with a measured sp^3 -bond content of 75% and a density of 2.7 g/cm^3 using a low voltage high current arc discharge [20].

To ensure all electrons pushed by the ponderomotive force of the laser may escape from the ions, the laser field E_L has to be larger than the electrostatic charge separation field E_s [6,16,21]. We normalize E_L to $E_0 = \omega_L m_e / e$ and find for the condition $a_L = E_L / E_0 \geq (n_e / n_c) k_L d$, where n_e is the electron density normalized to the critical density $n_c = \epsilon_0 m_e k_L^2 c^2 / e^2$, $k_L = 2\pi / \lambda_L$ and d the foil thickness. For a fully ionized DLC target as thin as 5 nm we find for a complete electron breakout $a_b = 23$, which is not far from the experimental condition.

Due to the remarkably high temporal laser contrast needed to investigate the described regime here, a low-

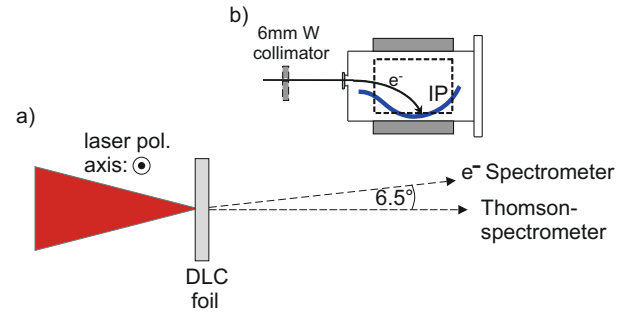


Fig. 1. (a) Experimental setup (top view): DLC foils were irradiated by linear polarized light in target normal configuration. Electrons were measured at 6.5° , while ions were diagnosed along target normal direction using a Thomson spectrometer. (b) A 6 mm thick Tungsten slit was used as collimator in front of the electron spectrometer which was equipped with an image plate (IP) as detector.

gain OPA pulse cleaning scheme has recently been implemented into the Trident laser system at the 250 μJ level [22]. Here, the initial pulse is split, where one beam is frequency doubled to use as pump, the other as seed signal in a subsequent OPA stage. The thus generated idler beam exhibits an inherent ultra-high contrast owing to the short pump pulse duration (500 fs). Pre-pulses and ASE-pedestal are efficiently suppressed within the pulse amplification due to the cubic relationship between idler and signal. The laser contrast on target was evaluated performing a target damage threshold measurement for both 500 fs and 1.2 ns pulses. Here, the target was imaged at its original shooting position and low energy pulses from the frontends were shot onto a DLC target. Clear target damage was found at 10^{11} W/cm^2 (500 fs) and 5×10^8 W/cm^2 (1.2 ns). Since we observed efficient ion acceleration in full power shots from DLC targets, we infer that the target was not destroyed before the main pulse due to insufficient laser pulse contrast. Hence, the intensity of potential pre-pulses and ASE pedestal must have been below the target damage threshold, resulting in an estimated lower limit for Trident laser contrast of 5×10^{-10} for pre-pulses and 2×10^{-12} for a ns ASE pedestal. These remarkable values enabled us to shoot ultra-thin DLC targets without using any additional plasma mirror setup [23,24].

The experimental configuration is shown in Figure 1. Electrons were measured with a permanent magnet electron spectrometer [25], installed at 6.5° with respect to target normal direction due to geometric constraints. A 6 mm thick Tungsten collimator with a 6 mm \times 0.3 mm horizontal slit in the center was mounted ~ 50 cm away from the target, giving a solid angle of $\sim 7 \times 10^{-6}$ sr. An image plate (Fujifilm: BAS-SR [26]) placed into the gap of the two magnets was used as detector. Image plates store information by stimulated phosphor centers which can be later on readout via the effect of photostimulated luminescence (PSL) using commercial scanners (here: Fujifilm FLA-7000). Their response to high energetic electrons has been extensively studied and is calibrated over a broad energy range [27,28]. From that work, we deduce a constant

calibration factor of 0.01 PSL/electron for electrons above 10 MeV. Owing to the fact that the image plate response is sensitive to the incidence angle of the electron signal [28], the detector was bent in such a way that this angle was held constant (10°) throughout the whole dispersion range (Fig. 1). As the recorded signal on image plates decreases in time, the detector was readout with a constant delay of 10 min after each shot. We account for the relatively fast signal fading during that time by multiplying the read out values by a factor of 4/3, found from the calibration curve in [28].

In addition to the electron diagnostic, ion energies were characterized along target normal direction, using a Thomson parabola spectrometer, positioned 1.2 m away from the target, and measuring within a solid angle of 5×10^{-8} sr. Ion tracks were recorded using 1 mm thick CR39 nuclear track detectors equipped with an additional image plate at the rear side. As high energetic ions result from electrostatic fields built up by hot electrons bound to the target, the measured ions are an important diagnostic for the electron dynamics. An efficient electron breakout from the target should result in a significant drop of the observed ion energies.

3 Results

In the presented experiment, DLC foil targets ranging from 58 nm down to 3 nm in thickness were used. In the following we discuss particle acceleration results from two target thicknesses, a 5 nm DLC foil nearly fulfilling the analytical condition for electron breakout as discussed above and a 42 nm DLC foil being an order of magnitude below this threshold. The resulting electron spectra are shown in Fig. 2a. The electrons measured from the 42 nm foil closely resemble a Maxwellian-like distribution, similar to what has been observed in previous work studying acceleration from targets in the μm thickness range [25]. The hot electron temperature can be deduced from an exponential fit and is found to be $k_B T = 12$ MeV.

In contrast, electrons generated from the interaction with a 5 nm foil exhibit very different characteristics. Here, a distinct quasi-monoenergetic feature, peaked at an energy of 30 MeV with 9 MeV rms spread is observed. The measured charge located within the rms limits of the electron peak is 7 pC. This number is remarkably high considering the fact that the spectrometer captured only a small fraction of the generated electron bunch owing to the limited observation angle of $\sim 7 \times 10^{-6}$ sr at 6.5° with respect to target normal direction. Therefore, we expect the total charge within the peak to be orders of magnitude higher. In addition, the total energy in the spectrum for electrons above 20 MeV has increased by more than a factor of 2.5 while decreasing the target thickness from 42 nm to 5 nm.

A strong correlation is seen when comparing the electron data with the simultaneously obtained ion spectra shown in Fig. 2b. When the foil thickness is decreased and the electron energy distribution evolves into a non-Maxwellian shape peaked at the highest energies, the corresponding cut-off values for the ions collapse. We

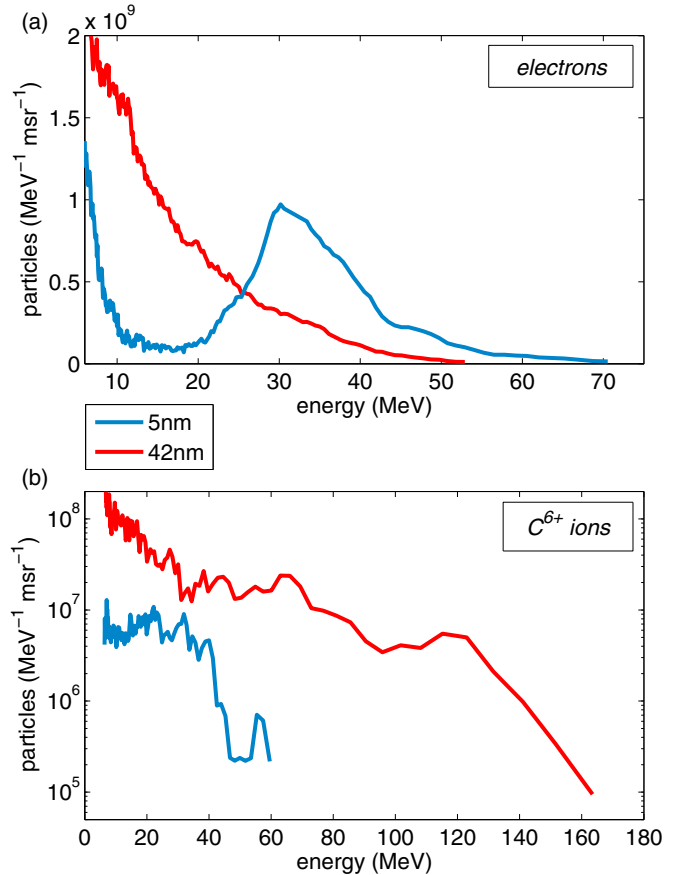


Fig. 2. Electron (a) and C^{6+} ion spectra (b) as observed from a DLC foil target of thickness 42 nm (marked in red) and 5 nm (illustrated in blue). The electron spectrometer was located at an angle of $\theta = 6.5^\circ$ with respect to target normal direction whereas ions were measured simultaneously at $\theta = 0^\circ$. While the 42 nm foil shows a Maxwellian-like distribution, a distinct quasi-monoenergetic peak is generated in the case of a 5 nm thick target. At the same time, the ion acceleration breaks down severely.

obtained maximum energies of 160 MeV for fully ionized carbon C^{6+} ions and 37 MeV protons for the shown 42 nm shot, dropping to 60 MeV and 19 MeV respectively for the discussed 5 nm case when electrons break out from the foil. The observed breakdown of efficient ion acceleration becomes even more dramatic when taking into account the total energy content in the measured ion spectra, which decreases by more than a factor of 20 when integrating over the whole spectrum compared to the 42 nm case.

4 Discussion

We observed a drastic change in the energy distribution of electrons from exponential to peaked when decreasing the target thickness from 42 nm down to 5 nm. At the same time, we find a substantial decrease in the ion cut-off energies as well as in the total energy in the ion spectrum.

For thick targets most of the electrons remain bound to the foil owing to their self-induced electric fields which in turn are responsible for efficient ion acceleration. However, going down to a target as thin as 5 nm we see a significant drop of ion energies while simultaneously a quasi-monoenergetic feature in the electron spectrum sets in. This behavior can be intuitively understood by the collapse of the longitudinal electric field accelerating the ions when a major fraction of the electron population is permanently separated from the foil. Thus, we attribute the observed features to the fact that a majority of electrons could escape from the ultra-thin target and state that the observation of the acceleration of ions provides a direct fingerprint for the regime of electron breakout.

This interpretation is supported by the fact that for the 5 nm foil the breakout condition $a_L \geq (n_e/n_c)k_L d$ is nearly fulfilled. It is important to note that this analytical expression gives an upper limit for the minimum a_L necessary for electron breakout since it represents the threshold where the ponderomotive force of the laser exceeds the restoring force induced by the *complete* charge separation field of *all electrons* from the ions. Additionally, the peaked spectral distribution gives evidence that the majority of the escaped electrons were accelerated in the same field. This experimental observation points towards a scenario, where all electrons in one bunch gain their energy within only one half-cycle of the laser pulse [6,14]. We note that due to the comparably long pulse duration used in the experiment and the consequently slowly rising laser amplitude, it is likely that not a single but a train of multiple electron bunches is generated, separated in time by $\Delta t = \pi/\omega_L = 1.8$ fs as it was shown in PIC simulations [29]. However, this process is restricted to only a few laser cycles by the limited number of electrons located within the focal volume. In contrast, for thicker, i.e. 42 nm targets the interaction dynamics is completely different. Here, the electrons remain bound to the target and are heated over many laser cycles, resulting in a broad energy distribution as seen in the experiment.

It is worth mentioning that for long pulses as used in the present experiment the initially thin foil will eventually expand prior to the arrival of the peak of the laser pulse even without the presence of pre-pulses. Nonetheless, the condition $a_L \sim (n_e/n_c)k_L d$ still remains fulfilled. This encourages our interpretation of electron breakout.

The observed electron spectrum at 5 nm target thickness is not yet directly understood. Assuming electron vacuum acceleration during one laser half-cycle at laser peak intensity ($a_L \approx 12$), we deduce a maximum electron energy $E_{max} = (1 + 2a_L^2)m_e c^2 \approx 150$ MeV [6], in contrast to the experimentally observed spectral maximum at 30 MeV, which would correspond to a somewhat reduced laser field amplitude of $\sim a_L/2$ within this model. Hence, the electron breakout may have occurred even before the laser peak intensity was reached, which may also follow from the given breakout condition if we assume a slight reduction of the normalized areal electron density owing to a small expansion of the target during the rise time of the laser pulse. Besides, it was shown that the final elec-

tron energy gain for a single electron in a tightly focused laser beam may be reduced for a given a_L [30,31]. However, in our case the back reaction of the electron bunch on the laser fields is rather strong. This will result in strong changes of the accelerating fields, but the general trend of a reduction of the electron energy may still occur. In addition, the induced charge separation field may also reduce the final energy of the ejected electrons.

As the measurement was restricted to a small observation angle located at an offset of 6.5° with respect to target normal (Fig. 1), the angular distribution of the accelerated electrons remains uncertain. In a simple picture of single electron acceleration within a half cycle of a plane wave at peak intensity a_L a deflection angle of the electrons along laser polarization direction given by $\Theta = \arctan(1/a_L) \approx 5^\circ$ is predicted [6]. However, when using a tightly focused laser beam as it was done in the conducted experiment, the quasi-plane wave approximation may not hold anymore, and it was shown that additional longitudinal fields in focus may become strong, leading to an isotropic ring structure of ejected electrons [32]. Therefore, we expect a significant number of electrons also being accelerated in the plane perpendicular to the laser polarization, which may explain the strong electron signal detected in the experimental configuration (Fig. 1). Besides, taking into account a spatially and temporally Gaussian shaped laser pulse as used in the presented experiment, plasma fields come into play and a more complex analysis is needed to describe the angular distribution.

It should be noted that electrons were detected at a large distance (1.2 m) with respect to the interaction region, and therefore Coulomb repulsion will lead to a spatial expansion of the initially highly dense electron bunch. However, this effect is significantly reduced taking into account the ultra-relativistic propagation [33].

To finally obtain the full Doppler boost $4\gamma^2 = 4/(1 - \beta^2)$ of backscattered photons from a relativistic electron mirror, it is important to orient the mirror surface normal to the electron velocity [11–13,34]. In particular, due to the transverse symmetry of the mirror, only the normal velocity $\beta_\perp = v_\perp/c$ is important whereas the parallel component $\beta_\parallel = v_\parallel/c$ does not contribute. Thus, the γ -factor of the mirror surface is $\gamma_s = 1/\sqrt{1 - \beta_\perp^2}$, and we obtain: $\gamma_s^2 = 1/(1 - \beta_\perp^2) = 1/(1 - \beta^2 + \beta_\parallel^2) = 1/(\gamma^{-2} + \beta_\parallel^2)$. Thus, $\gamma_s \simeq \gamma$ only if $\gamma^{-1} \geq \beta_\parallel$ and β_\parallel really has to be small for larger γ values. This can be obtained by correspondingly tilting the target and (or) tilting the laser pulse front [35]. Therefore, tilting the relativistic mirror to an angle such that the electron velocity angle crosses the mirror angle during the final acceleration may be experimentally easy to achieve but has to be considered to reach the full $4\gamma^2$ Doppler boost.

It is very time consuming to study the breakout and vacuum acceleration of electron bunches in two-dimensional particle-in-cell (PIC) simulations, as the small foil thickness requires very small cell sizes and at the same time the energy gain of the electrons during a laser half cycle in the electron rest frame, corresponds to

many laser wavelength in the laboratory system. Also the long laser pulse studied in small time steps takes long computing times. Thus, we could not finish such calculations when submitting this publication, but they should clarify our understanding.

5 Outlook

Highly brilliant X-ray sources experience a strong demand in a variety of different fields. Here, coherent Thomson backscattering may provide a compact technique to obtain ultra-short X-ray pulses within a largely tunable range, suitable for research and medical applications. For instance, the coherent scattering of 1.5 eV photons off a relativistic electron sheet propagating at an energy of 30 MeV would result in an ultra-short 20 keV X-ray pulse, giving single molecule imaging a powerful light source, whereas 40 keV coherent X-rays as requested for medical applications could be generated off a 42 MeV electron sheet. Additionally, industrial applications like lithography may come into reach.

In future experiments, a more elaborate electron diagnostic is foreseen to obtain a detailed picture of the electron sheet dynamics. In a second step, this relativistic electron mirror will be used for first measurements towards coherent Thomson backscattering. For such experiments, ultrathin DLC foils are well suited as target material due to their excellent properties in terms of chemical inertness as well as mechanical stability and radiation hardness. Compared to single layer graphene [14,36], sp^3 -bonded few layer diamond is more tolerable to imperfections in the laser contrast, which is absolutely necessary for high power laser applications. So far, our target fabrication facility is capable of producing highly stable DLC foils as thin as 3 nm. To extend the range of target thicknesses available, we are currently developing techniques to produce even thinner foils with reduced roughness. This will enable the generation of laser-driven relativistic electron mirrors also at systems limited to a somewhat smaller normalized vector potential a_L . It is very clear that few cycle, high-contrast, intense laser pulses are best for the acceleration of the high density electron sheets from DLC-foils. Circular polarized laser light may be better than linear polarized light to avoid any heating of electrons during the short rise time of the laser pulse [37].

We acknowledge many useful discussions with J. Meyer-ter-Vehn, H.-C. Wu, X.Q. Yan, S. Rykovanov, B. Qiao, M. Geissler, H. Ruhl, and T.E. Cowan for providing the electron spectrometer. This work was performed under the auspices of the US DOE and was supported by the LANL Laboratory Directed Research and Development (LDRD) program and by the DFG under Contract No. TR18 and the DFG cluster of excellence Munich-Centre for Advanced Photonics. D. Kiefer, A. Henig and D. Jung acknowledge financial support from the International Max-Planck Research School on Advanced Photon Science (IMPRS-APS), J. Schreiber from the German

Academic Exchange Service (DAAD). The authors acknowledge the support by the European Commission under contract ELI pp 212105 in the framework of the program FP7 Infrastructures-2007-1.

References

1. J. Faure, Y. Glinec, A. Pukhov, S. Kiselev, S. Gordienko, E. Lefebvre, J.-P. Rousseau, F. Burgy, V. Malka, *Nature* **431**, 541 (2004)
2. S.P.D. Mangles, C.D. Murphy, Z. Najmudin, A.G.R. Thomas, J.L. Collier, A.E. Dangor, E.J. Divall, P.S. Foster, J.G. Gallacher, C.J. Hooker, D.A. Jaroszynski, A.J. Langley, W.B. Mori, P.A. Norreys, F.S. Tsung, R. Viskup, B.R. Walton, K. Krushelnick, *Nature* **431**, 535 (2004)
3. C.G.R. Geddes, C. Toth, J. van Tilborg, E. Esarey, C.B. Schroeder, D. Bruhwiler, C. Nieter, J. Cary, W.P. Leemans, *Nature* **431**, 538 (2004)
4. S. Kneip, S.R. Nagel, C. Bellei, N. Bourgeois, A.E. Dangor, A. Gopal, R. Heathcote, S.P.D. Mangles, J.R. Marques, A. Maksimchuk, P.M. Nilson, K.T. Phuoc, S. Reed, M. Tzoufras, F.S. Tsung, L. Willingale, W.B. Mori, A. Rouse, K. Krushelnick, Z. Najmudin, *Phys. Rev. Lett.* **100**, 105006 (2008)
5. A. Einstein, *Ann. Phys.* **17**, 891 (1905)
6. D. Habs, M. Hegelich, J. Schreiber, M. Gross, A. Henig, D. Kiefer, D. Jung, *Appl. Phys. B* **93**, 349 (2008)
7. A.V. Panchenko, T.Z. Esirkepov, A.S. Pirozhkov, M. Kando, F.F. Kamenets, S.V. Bulanov, *Phys. Rev. E* **78**, 056402 (2008)
8. M. Kando, Y. Fukuda, A.S. Pirozhkov, J. Ma, I. Daito, L.-M. Chen, T.Z. Esirkepov, K. Ogura, T. Homma, Y. Hayashi, H. Kotaki, A. Sagisaka, M. Mori, J.K. Koga, H. Daido, S.V. Bulanov, T. Kimura, Y. Kato, T. Tajima, *Phys. Rev. Lett.* **99**, 135001 (2007)
9. A.S. Pirozhkov, J. Ma, M. Kando, T.Z. Esirkepov, Y. Fukuda, L.-M. Chen, I. Daito, K. Ogura, T. Homma, Y. Hayashi, H. Kotaki, A. Sagisaka, M. Mori, J.K. Koga, T. Kawachi, H. Daido, S.V. Bulanov, T. Kimura, Y. Kato, T. Tajima, *Phys. Plasmas* **14**, 123106 (2007)
10. B. Dromey, S. Kar, C. Bellei, D.C. Carroll, R.J. Clarke, J.S. Green, S. Kneip, K. Markey, S.R. Nagel, P.T. Simpson, L. Willingale, P. McKenna, D. Neely, Z. Najmudin, K. Krushelnick, P.A. Norreys, M. Zepf, *Phys. Rev. Lett.* **99**, 085001 (2007)
11. T. Baeva, S. Gordienko, A. Pukhov, *Phys. Rev. E* **74**, 046404 (2006)
12. T. Baeva, *High harmonic generation from relativistic plasma*, Ph.D. thesis, 2008
13. A. Pukhov, T. Baeva, D. an der Brügge, S. Münster, *Eur. Phys. J. D* **55**, 407 (2009)
14. V.V. Kulagin, V.A. Cherepenin, M.S. Hur, H. Suk, *Phys. Rev. Lett.* **99**, 124801 (2007)
15. B. Rau, T. Tajima, H. Hojo, *Phys. Rev. Lett.* **78**, 3310 (1997)
16. O. Klimo, J. Psikal, J. Limpouch, V.T. Tikhonchuk, *Phys. Rev. ST Accel. Beams* **11**, 031301 (2008)

17. D. Habs, F. Grüner, U. Schramm, P. Thirolf, M. Sewtz, S. Becker, AIP Conf. Proc. **802**, 6 (2005)
18. F. Grüner, S. Becker, U. Schramm, T. Eichner, M. Fuchs, R. Weingartner, D. Habs, J. Meyer-ter-Vehn, M. Geissler, M. Ferrario, L. Serafini, B. Van der Geer, H. Backe, W. Lauth, S. Reiche, Appl. Phys. B **86**, 431 (2007)
19. K.A. Flippo, J. Workman, D.C. Gautier, S. Letzring, R.P. Johnson, T. Shimada, Rev. Sci. Instrum. **79**, 10E534 (2008)
20. V.K. Liechtenstein, T.M. Ivkova, E.D. Olshanski, I. Feigenbaum, R. DiNardo, M. Dbeli, Nucl. Instrum. Meth. A **397**, 140 (1997)
21. T. Esirkepov, M. Borghesi, S.V. Bulanov, G. Mourou, T. Tajima, Phys. Rev. Lett. **92**, 175003 (2004)
22. R.C. Shah, R.P. Johnson, T. Shimada, K.A. Flippo, J.C. Fernandez, B.M. Hegelich, Opt. Lett., in press
23. C. Thauray, F. Quéré, J.-P. Geindre, A. Levy, T. Ceccotti, P. Monot, M. Bougeard, F. Réau, P. d'Oliveira, P. Audebert, R. Marjoribanks, P. Martin, Nat. Phys. **3**, 424 (2007)
24. A. Henig, D. Kiefer, K. Markey, D.C. Gautier, K.A. Flippo, S. Letzring, R.P. Johnson, T. Shimada, L. Yin, B.J. Albright, K.J. Bowers, J.C. Fernandez, S.G. Rykovanov, M. Zepf H.-C. Wu, D. Jung, V.K. Liechtenstein, Phys. Rev. Lett., in press
25. T.E. Cowan, M.D. Perry, M.H. Key, T.R. Ditmire, S.P. Hatchett, E.A. Henry, J.D. Moody, M.J. Moran, D.M. Pennington, T.W. Phillips, T.C. Sangster, J.A. Sefcik, M.S. Singh, R.A. Snavely, M.A. Stoyer, S.C. Wilks, P.E. Young, Y. Takahashi, B. Dong, W. Fountain, T. Parnell, J. Johnson, A.W. Hunt, T. Kühl, Laser Part. Beams **17**, 773 (1999)
26. <http://www.fujifilm.com/products>
27. B. Hidding, G. Pretzler, M. Clever, F. Brandl, F. Zamponi, A. Lubcke, T. Kampfner, I. Uschmann, E. Forster, U. Schramm, R. Sauerbrey, E. Kroupp, L. Veisz, K. Schmid, S. Benavides, S. Karsch, Rev. Sci. Instrum. **78**, 083301 (2007)
28. K.A. Tanaka, T. Yabuuchi, T. Sato, R. Kodama, Y. Kitagawa, T. Takahashi, T. Ikeda, Y. Honda, S. Okuda, Rev. Sci. Instrum. **76**, 013507 (2005)
29. Y. Tian, W. Yu, P. Lu, H. Xu, V. Senecha, A. Lei, B. Shen, X. Wang, Phys. Plasmas **15**, 053105 (2008)
30. K.I. Popov, V.Y. Bychenkov, W. Ruzmus, R.D. Sydora, Phys. Plasmas **15**, 013108 (2008)
31. S.G. Bochkarev, V.Y. Bychenkov, Quantum Elec. **37**, 273 (2007)
32. B. Quesnel, P. Mora, Phys. Rev. E **58**, 3719 (1998)
33. *Classical Electrodynamics*, edited by J.H. Jackson (Wiley, New York, 1972)
34. J. Meyer-ter-Vehn, H.C. Wu, Eur. Phys. J. D **55**, 433 (2009)
35. G. Pretzler, A. Kasper, K.J. Witte, Appl. Phys. B **70**, 1 (2000)
36. K.S. Novoselov A.K. Geim, Nature Mater. **6**, 183 (2007)
37. S.G. Rykovanov, J. Schreiber, J. Meyer-ter-Vehn, C. Bellei, A. Henig, H.C. Wu, M. Geissler, New J. Phys. **10**, 113005 (2008)